International Journal of Ambient Computing and Intelligence

April-June 2011, Vol. 3, No. 2

Table of Contents

Editorial Preface

Research Articles

An Antiwindup Approach to Power Controller Switching in an Ambient Healthcare Network

Michael J. Walsh, University College Cork, Ireland

John Barton, University College Cork, Ireland

Brendan O'Flynn, University College Cork, Ireland

Martin J. Hayes, University of Limerick, Ireland

Cian O'Mathuna, University College Cork, Ireland

Seyed Mohammad Mahdi Alavi, Simon Fraser University, Canada

ABSTRACT

This paper proposes a methodology for improved power controller switching in mobile Body Area Networks operating within the ambient healthcare environment. The work extends Anti-windup and Bumpless transfer results to provide a solution to the ambulatory networking problem that ensures sufficient biometric data can always be regenerated at the base station. The solution thereby guarantees satisfactory quality of service for healthcare providers. Compensation is provided for the nonlinear hardware constraints that are a typical feature of the type of network under consideration and graceful performance degradation in the face of hardware output power saturation is demonstrated, thus conserving network energy in an optimal fashion.

Keywords: *Anti-Windup, Bumpless Transfer, Hardware Constraints, Power Controller Switching, Wireless Networks*

1. INTRODUCTION

Ubiquitous or pervasive Body Area Networks (BANs) and their use in the healthcare application space are now beginning to reach a level of maturity wherein a number of innovative solutions are now at advanced stages of commercial development. Several projects, for instance the Complete Ambient Assisted Living Experiment (CAALYX) (Boulos et al., 2007) and Codeblue (Gao et al., 2008), are now actively promoting advances in technology and infrastructure that facilitate independent living, pre-hospital and in-hospital emergency care and disaster response. New hardware technologies, including a number of state of the art sensor node platforms, (e.g. Tmote, Mica, Micaz and more recently Sentilla), are being adapted

DOI: 10.4018/jaci.2011040103

for deployment in applications where human wellness maintenance is actively addressed. A number of themes are emerging in this pre-competitive phase of development:

- The quality of the service provided to both the user and to the health care provider is crucial in terms of maximising BAN market penetration.
- Although some guaranteed level of information flow is a clear necessity for service provision factors such as energy consumption, battery life and size are proving to be just as important factors when it comes to increasing the uptake of new services and systems.
- In community health care settings support for some level of ambulatory motion must be provided without any technical concerns about information loss being a factor.
- Some hardware limitations will inevitably be a feature of the BAN devices that are worn by the user. These limitations should have no impact on the quality of service that is provided. In short BAN devices and systems should be Robust, power aware, mobile, and low cost and be readily implementable in a health care environment. This paper illustrates how these challenges can be addressed using recent developments in the area of systems science. In particular it is shown how Anti-Windup (AW) and Bumpless Transfer (BT) techniques can be applied to the design of next generation BANs that can address the aforementioned issues in an optimal fashion. Although the processing of relevant biometric information can consume valuable energy, it is clear that data transmission is the primary constraint on battery life in a BAN and can account for 70-90% of power usage (Ares et al., 2007). The benefits of transmission power control are obvious when there exists a need for the BAN to remain operational for extended periods of time and to this end a number of wireless network power control algorithms have already been proposed (Walsh et al., 2008; Alavi et al., 2008, Walsh et al., 2009, Alavi et al., 2010, Subramanian et al., 2005, Chen et al., 2006). These schemes have exhibited some success in extending battery lifetime while concurrently providing pre-specified levels of quality of service (QoS). This equates to the provision of sufficient data to reassemble biometric waveforms, (e.g. ECK, EEG, blood oxygen levels, pulse ect.), or to reliably detecting the movement of an elderly person, in an ambient fashion, be they at home or in a care facility.

A. Remark: Practical Measurement of QoS for Dynamic Control

In this work QoS will be taken to mean an accurately tracked received signal strength (RSS) target value thereby guaranteeing a bit error rate that is below a certain predefined threshold level. There exists a body of opinion suggesting that RSS is not a suitable metric for this task, largely based on the random variability that has been observed in past mobility experiments. However this work provides practical evidence that the more stable radios that are now a feature of the 802.15.4 market can provide a basis for real time control. In this regard, the results presented here complement the claims made by a number of respected authors in defense of RSS (Ares, 2007). Moreover, no new point of principle arises in the use of any other practicable real time performance metric for BAN purposes, if and when one comes to hand.

2. PERFORMANCE CONSTRAINTS IN A TYPICAL BODY AREA NETWORK

A variety of limits on performance surface sooner rather than later in a practical BAN. This section outlines the constraints that are treated by this work.

Figure 1. The ambient healthcare environment where power control for X is initially handled by BS1 . Subject X then moves in an ambulatory fashion and switching occurs between BS1 and BS2 . Data is now multihopped via BS2 to BS1 and BS2 handles power control for X. Hence power controller switching has occurred between BS1 and BS2.

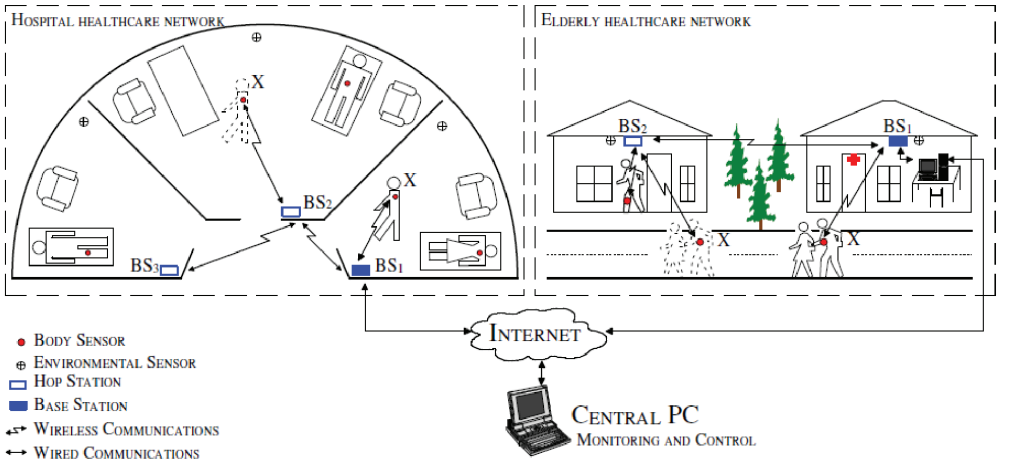

A. Hardware Limitations

When employing embedded systems in miniaturised BAN applications a number of hardware related factors are an inevitable constraint on performance. For instance the limited, necessarily quantised, and quite often saturated transceiver output power of a typical mobile node can severely degrade network performance, ultimately leading to instability if not properly addressed. In this work Anti-Windup (AW) control is shown to demonstrate graceful BAN performance degradation in the face of such constraints. AW actively seeks to minimise controller gain and also exhibits improved network energy consumption. This paper provides a novel practical example of how to address these types of unavoidable nonlinear constraints in an optimal fashion.

B. Network Coverage

Another major challenge lies in maximizing network coverage area. Given that many of the "off-the-shelf" sensor node platforms operate using low power 802.15.4 type wireless technolo-gies, transmission range is extremely limited, especially in the indoor environment. A multihop or mesh network topology is often proposed to extend coverage area necessitating the introduction of a switching protocol that is power aware. Figure 1 illustrates the type of scenario that is envisaged whereby subject X is being monitored and is wearing (perhaps a number of) wireless biometric devices. Initially X is in communication with base station BS_1. When X moves to an adjoining area in an ambulatory fashion, data must at some point be transmitted via BS_2 rather than BS_1 quite possibly within a mesh paradigm. It is crucial that the QoS and energy efficient properties of the BAN be retained in such a scenario. Here "bumpless transfer" (BT), (Hanus et al., 1987), is employed to optimise this process. In the proposed BT scheme a global controller oversees multiple local loop controllers that are designed to ensure that the mesh is power aware. Depending on certain performance requirements, a sequence of switches is necessary between each controller. In essence, one controller will be operational or "on-line" while the other candidate controller(s) must be deemed "off-line" at any instant.

Clearly it is necessary to be able to switch between these controllers (located at adjacent base stations) in a stable fashion. This paper presents sufficient conditions to ensure that the induced transient signals are bounded, thereby satisfying network stability requirements. To achieve this smoothly, the gap between the off and online control signals must be bounded so that the control signal driving the plant cannot induce instability.

In this work both AW and BT are applied in tandem for the first time in a practical network, thereby providing effective control of the signal entering the 'plant' (in this case the node transceiver) at any instant For the remainder of the work the term anti-windup-bumpless-transfer or AWBT is coined to denote the new technique.

This work addresses the nonlinear elements outlined above in a power control setting that is both QoS energy efficient. The necessary extensions that are required to AWBT results to account for challenges posed by wired and wireless communications are also presented. In the first instance the problem is treated for the 2 base station scenario and is subsequently extended to the general case. Traditional AWBT schemes require that the gap between the feedback measurement observed at the "off-line" controller(s), is(are) sufficiently close in magnitude to that observed at the "on-line" controller. The particular constraints imposed by the use of practical devices and in particular the use of the received signal strength (RSS) as the tracking signal observed at each successive base station is considered in detail. To this end a specific modification is proposed that delivers an AWBT scheme capable of compensate for the differing feedback signals that naturally arise in the problem at hand.

3. FORMAL STATEMENT OF THE CONTROLLER SWITCHING PROBLEM: TWO BASE STATION SCENARIO

To determine when switching should occur the filtered downlink received signal strength indicator (RSSI) signal or the RSSI signal is considered at the mobile node. It is assumed that each base station or access point will possess the ability to transmit at a predefined maximum power level within some quantisation structure at any instant. Initially, the two node mobile ad-hoc WSN scenario depicted in Figure 2(a) is considered. When the network initializes it is assumed that the Mobile Node (MN) is unaware of its position and is transmitting data using maximum transmission power to all "listening" base stations Figure 2(a)(i).

The network connects and implements power controller switching as per Figure 2(b). The MN will subsequently receive data packets from each base station within range (in this scenario limited to BS1 and BS2). A downlink RSSI is now calculated for each received packet and this signal is subsequently filtered to remove any multipath or high frequency component, using a digital low pass filter, *F(z)*. The average speed at which the mobile node travels when considered with the environmental conditions influence the selection of the filter's parameters. Stemming from this the higher the speed and the density of sensor nodes, the lower the cut of frequency that is required. In the experiment presented in this work the filter:

$$F(z) = \frac{0.25z}{z - 0.75} \tag{1}$$

was found to be satisfactory. Figure 3 illustrates how, subsequent to filtering the downlink RSSI signal, the pathloss component remains. This element is shown here, and earlier by other authors (Goldsmith, 2006), to be sufficiently distance dependant to be useful for real time control. The MN now executes the algorithm presented in Table 1 comparing the resultant filtered signals, $RSSI_{DownlinkBS\ 1}$ and $RSSI_{DownlinkBS\ 2}$ over three sample periods. The signals are also compared with a predefined threshold value, selected here to be -40 dBm. This threshold ensures that the base station is located in the highest possible tier of the BAN hierarchy and is also within range of the mobile

Figure 2. (a) Simple WSN multihop scenario. (b) The power controller switching procedure based on filtered downlink RSSI.

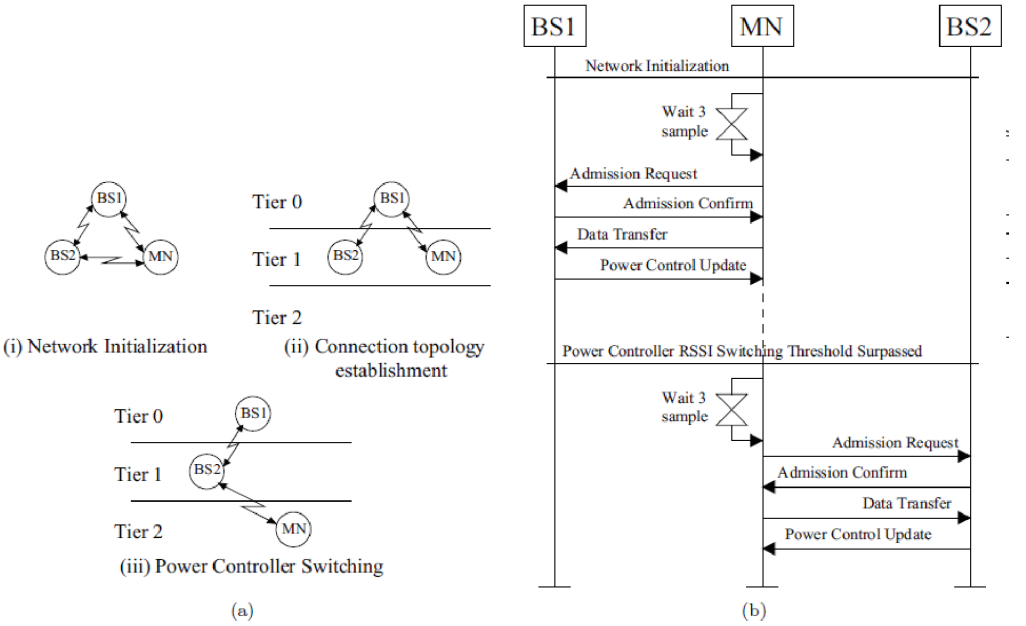

node that will have routing precedence, thereby satisfying a minimal latency requirement within the network.

An admission request is then sent to the base station whose downlink RSSI satisfies the switching criteria (*BS1* following network initialization). Following confirmation the mobile node implements any power level updates received from this base station. Filtering the RSSI provides the added advantage of preventing chatter, i.e., occurring too frequently, caused by any deep fades in the RSSI that may be a characteristic of the *MN* position at any instant. Furthermore the three sample period delay prior to sending an admission request ensures that jitter is not present in the system.

From Figure 2(a)(ii) and following network initialization, *MN* is now located in tier 1 of the mesh hierarchy and *BS1*, located in tier 0, dynamically manages the *MN's* power based on the uplink RSSI observed at *BS1*. At some future sampling instant, due to *MN* mobility, power controller switching is required based on the algorithm of Table 1, again by a consideration of the filtered downlink RSSI values, $RSSI_{DownlinkBS\,1}$ and $RSSI_{DownlinkBS\,2}$ and the threshold value -40 dBm. Subsequently *MN* joins tier 2 in the hierarchy, see Figure 2(a)(iii) and power control for *MN* is now implemented through the uplink RSSI at BS2.

4. MODELLING THE NETWORK

The goal of this work is to dynamically adjust the mobile node transmitter power in a distributed manner, so that the power consumption is minimized while also maintaining sufficient transmission quality. A direct measurement of QoS is therefore an a priori requirement. In the past it has been suggested that uplink RSSI was a less than ideal metric for power control, however this claim was based on experimentation with early platforms using older radios, e.g. the Texas

Figure 3. Received signal strength filtered using (1) to remove the high frequency component

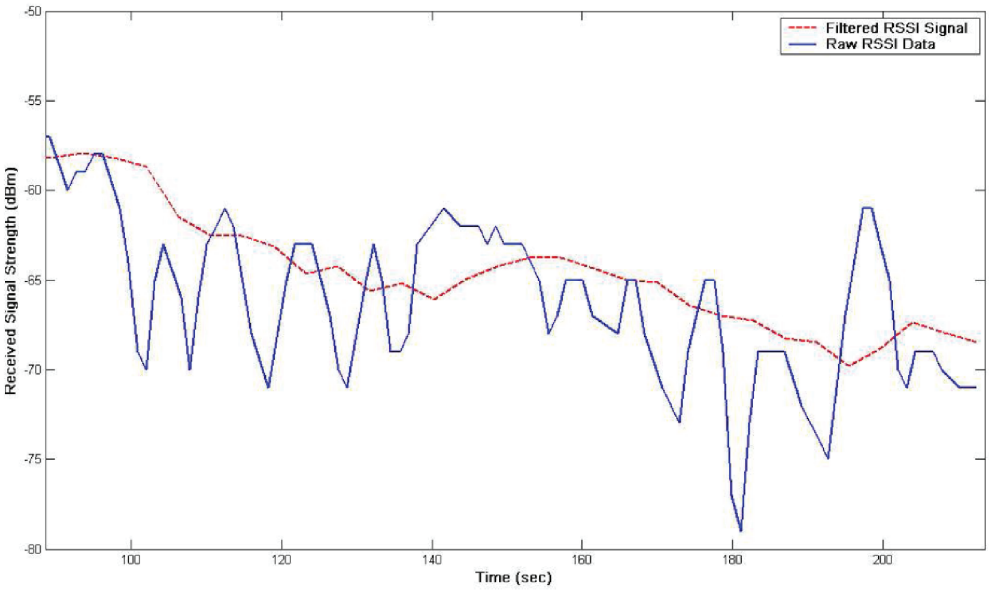

Table 1. Pseudo code for power controller switching algorithm: 2 base station example

Base Station 1 (BS1 located in tier 0)
Network Initialization
0 Downlink RSSI for BS1 recorded at MN 1 For number of sample periods = 1 to 3 2 If $RSSI_{DownlinkBS\ 1} > RSSI_{DownlinkBS\ 2}$
3 Or If $RSSI_{DownlinkBS\ 1} > -40dBm$
4 Use power level updates from Base Station 1

Base Station 2 (BS2 located in tier 1)
Network Initialization
0 Downlink RSSI for BS2 recorded at MN 1 For number of sample periods = 1 to 3 2 If $RSSI_{DownlinkBS\ 2} > RSSI_{DownlinkBS\ 1}$
3 And If $RSSI_{DownlinkBS\ 1} < -40dBm$
4 Use power level updates from Base Station 2

Instruments CC1000, where hardware miscalibration or drift was often a problem. More recently newer 802.15.4 compliant radios such as the TI CC2420, have been shown to exhibit highly stable performance and it is now commonly held that for a given link, RSSI exhibits acceptably small time-variability (Srinivasan et al., 2006). In this work the received signal strength indicator (RSSI) is therefore selected as the feedback variable to manage the control objective.

In Ares et al. (2007) a method was introduced to directly estimate the signal to noise plus interference ratio (SINR) using RSSI measurements. The SINR $\gamma(k)$, in terms of RSSI is given by:

$$\gamma(k) \approx RSSI(k) - n(k) - C - 30 \quad (2)$$

where the addition of the scalar term 30 accounts for the conversion from dBm to dB, $n(k)$ is thermal noise and C is the measurement offset assumed to be 45 dB.

A setpoint or reference RSSI value can therefore be selected and related directly to *PER*, as outlined in the 802.15.4 standard (In-

ternational Organization for Standardization, 2007). To expand, the bit error rate (BER) for the 802.15.4 standard operating at a frequency of 2.4GHz is given by:

$$BER = \frac{8}{15} \times \frac{1}{16} \times \sum_{k=2}^{16} -1^{k} \begin{pmatrix} 16 \\ k \end{pmatrix} e^{20 \times SINR \times (\frac{1}{k} - 1)} \tag{3}$$

and given the average packet length for this standard is 22 bytes, the PER can be obtained from:

$$PER = 1 - (1 - BER)^{PL} \tag{4}$$

where *PL* is packet length including the header and payload. *PER* is more useful here given the transceiver used to practically implement the proposed methodology, is a wideband transceiver, transmitting and receiving data in packet rather than bit format. Establishing a relationship between *RSSI, SINR, BER* and subsequently *PER* can therefore help to prespecify levels of system performance.

A. The System Model

A systems science representation of a single base station communicating to a single mobile node is illustrated in Figure 4. The system has reference input *r(k)* (reference RSSI), the value for which is determined using (2), (3) and (4) above, guaranteeing a predefined PER. q(k) is quantization noise introduced as a result of switching between discrete power levels. The controller *K (z)* has controller output *u(k)* and takes the form *K (z) = [K_1 (z) K_2 (z)]* a standard two degree of freedom structure.

The plant *G(z)* is represented by *G(z) = [G_1 (z) G_2 (z)],* where G_1 *(z)* and G_2 *(z)* are the disturbance feedforward and feedback parts of G(z) respectively. Given no structured disturbance model is available in the form of a transfer function, $G_1(z)$ is taken to be $G_1 = I$, where *I* is the identity matrix. $G_2(z)$ is a low pass filter with sufficient bandwidth to eliminate quantization noise. $G_2(z)$ is selected as:

$$G(z) = \frac{1}{1.1z - 0.9} \tag{5}$$

$G_2(z)$ outputs a power level update *p(k),* which in turn is transmitted to the mobile node. The mobile node transmitter has inherent upper and lower bounds on hardware transmission power output, represented in Figure 4 by the saturation block, the output for which is saturated output power or p_m *(k).* H represents the hardware switch in the mobile node's transceiver and is taken here to be the identity matrix or *H = I.d(k)* is a disturbance to the system and comprises of channel attenuation, interference and noise.

B. Mapping the Saturation Function

For this scenario a problem presents itself in that the saturation constraint is located at the output of the system and while there have been some advances in control design theory to deal with this type of output constraint (Turner et al., 2007), there is a vast literature covering the treatment of linear systems subject to input saturation constraints (Bernstein et al., 1995) and references therein. A solution therefore lies in the mapping of the output saturation constraint to the input of the plant or the output of the controller. The saturation function is defined as:

$$p_m(k) = sat(p(k)) \tag{6}$$

where $sat(p(k)) := sign(p(k)) \times min\{|p(k)|, p_m(k)\}$ and where $p_m(k)$ is the output power saturation limit. Note the *sat(.)* function in (6), belongs to sector *[0, 1]* and is assumed locally Lipschitz. The following set is defined:

$$P := [-p_m(k), p_m(k)] \tag{7}$$

Where $sat(p(k) = p(k), \forall p(k) \in \mathrm{P}$. This is the set in which the saturation behaves linearly i.e. if there is no saturation present $p(k) = p_m(k)$ and the nominal closed loop system conditions are exhibited. Figure 5 portrays the system with the saturation block mapped from

Figure 4. Wireless System Model with saturation block at the output

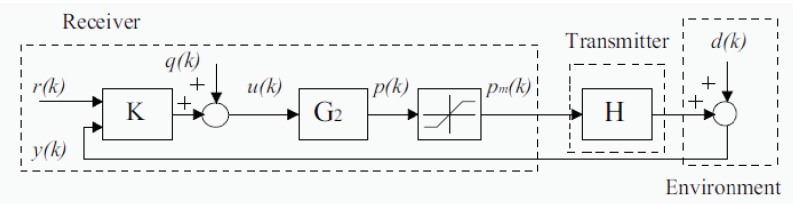

the output of the system to the input where $u_m(k)$ is the input to the plant. To represent the mapped saturation function we define the new set:

$$U = \left[\frac{\overline{-p_m(k)}}{h_{G_2}}, \frac{\overline{p_m(k)}}{h_{G_2}} \right] \quad (8)$$

where h_{G2} is the gain of the transfer function G_2. Recent advances in the anti-windup literature can now be applied to the problem at hand, ensuring minimal performance degradation during saturation and speedy recovery following saturation.

C. The Power Controller Switching Problem

Figure 6 illustrates the power controller switching problem for a two base station, one mobile node scenario. K_{BS1} and K_{BS2} are the same construct as $K(z)$ from the previous section. Basestation 1 is deemed "on-line" and is therefore controlling the mobile node's transmission power. The difficulty in switching between base station 1 and base station 2 is as a result of the possible difference between $p_1(k)$ and $p_2(k)$ at the time of switching. This discrepancy can exist due to incompatible initial conditions and can induce an unwanted transient and possible instability in the system. The result can be a disruption of vital health status data or indeed a loss in service altogether.

1) Conditions for stable switching:
   Assumption 1: As the work here is seeking global results, we are necessarily forced to assume that $G(z)$ is asymptotically stable. To expand given $G_2 \sim (A_p, B_p, C_p, D_p)$ in state space format and $H(z)$ is the identity matrix, if $|\lambda_{max}(A_p)| < 1$, where λ_{max} is the maximum eigenvalue, then asymptotically stable is guaranteed.
   Assumption 2: We also assume that the poles of $(1 - K_{BS1} G_2 H)(z)$ and $(1 - K_{BS2} G_2 H)(z)$ are in the open unit disc, ensuring both nominal closed loops are stable. When the above two necessary conditions are met then the stability of the switched system will be guaranteed if the control signals, $u_{m1}(k)$ and $u_{m2}(k)$ are sufficiently close to each other, thus an AWBT approach provides a stable solution to the power controller switching problem. $p_1(k)$ will therefore be close enough to $p_2(k)$ and should switching occur, a large unwanted transient will not be induced in the system. However an additional difficulty arises that is unique to the wireless case. As mentioned previously, in order for AWBT to be effective, the feedback measurement observed at the "off-line" controller must be sufficiently close in magnitude to the feedback measurement observed at the "on-line" controller. Clearly from Figure 6 $d_1(k) = d_2(k)$ due to differing propagation environments. This disparity can mean AWBT is unable to eliminate the difference between $u_{m1}(k)$ and $u_{m2}(k)$.

Figure 5. Wireless System Model with saturation block mapped from the output to the input of the system

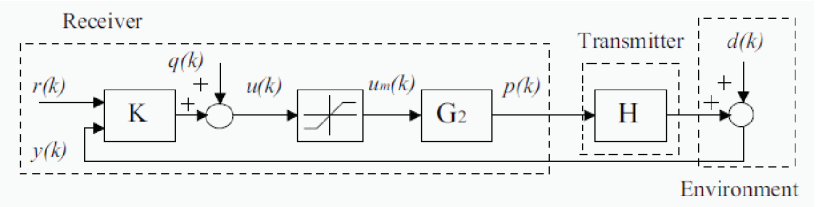

Figure 6.Wireless System Model with power controller switching

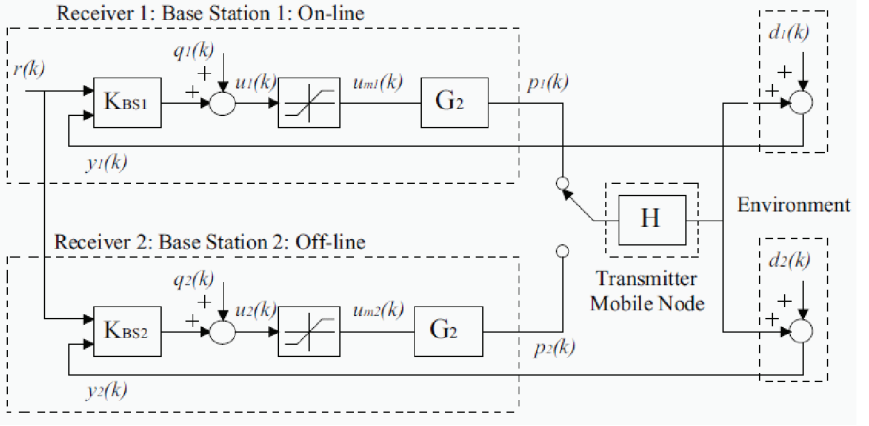

A more complex control design solution is therefore required. However prior to solving this, a linear controller must be synthesized. This controller provides pre-specified levels of stability and performance in the nominal linear closed loop i.e. when neither saturation nor switching is occurring. Following this a conservative anti-windup design is used to address the hardware saturation constraint. Finally a modification is made to the AWBT scheme to account the differing feedback signals and to enable seamless power controller switching.

5. ANTI-WINDUP DESIGN

The technique employed here implements a two step AWBT design procedure. The first step is to design a linear power controller ignoring the inherent nonlinear constraints on the system. The control design approach adopted here is based on quantitative feedback theory (QFT) and provides both robust stability and nominal performance in the linear operational region. The second step involves using recent advances in AW theory, to minimize degradation in the face of actuator constraints. The technique employed here is the Weston-Postlethwaite AntiWindup Bumpless Transfer (WP-AWBT) synthesis technique. First presented in (Weston et al., 1998) and later in its discretized form in (Herrman et al., 2006), this approach uses an L_2 approach in conjunction with linear matrix inequality (LMI) optimization techniques to ensure that during saturation the systems performance remains as close to nominal linear operation as possible and returns to the linear operational region as quickly as possible.

A. Robust Linear Power Tracking Controller Design

Quantitative feedback theory (QFT) provides an intuitively appealing means of guaranteeing both robust stability and performance and is essentially a Two-Degree-of-Freedom (2DOF) frequency domain technique, as illustrated in Figure 6 and detailed in (Borghesani et al., 2003) and (Horowitz, 2001). The scheme achieves client-specified levels of desired performance over a region of parametric plant uncertainty, determined a priori by the engineer. The methodology requires that the desired time-domain responses are translated into frequency domain tolerances, which in turn lead to design bounds in the loop function on the Nichols chart. In a QFT design, the responsibility of the feedback compensator, $K_2(z)$, is to focus primarily on attenuating the undesirable effects of uncertainty, disturbance and noise. Having arrived at an appropriate $K_2(z)$, a pre-filter $K_1(z)$, is then designed so as to shift the closed-loop response to the desired tracking region, again specified a priori by the engineer. The approach requires that the designer select a set of desired specifications in relation to the magnitude of the frequency response of the closed-loop system, thusly achieving robust stability and performance. The design procedure in its entirety is omitted here due to space constraints, however the interested reader is directed to (Walsh et al, 2010) where a detailed description is contained. Using this techniques outlined therein $K_2(z)$ was found to be:

$$K_2(z) = \frac{\text{z-0.6622}}{\text{0.7103z - 0.7103}} \tag{9}$$

guaranteeing a phase and gain margin equal to 50° and 1.44, respectively. The closed-loop transfer function is shaped using $K_1(z)$ ensuring the system achieves steady state around the target value of $5 \le t_{ss} \le 25(s)$ and a damping factor of $\xi = 0.5$ is selected to reduce outage probability at the outset of communication. The resultant $K_1(z)$ is:

$$K_1(z) = \frac{\text{1.4127z}}{\text{z - 0.4127}} \tag{10}$$

B. WP-AWBT Synthesis

Consider the generic AW configuration shown in Figure 7(a). As illustrated above the plant takes the form $G = [G_1\ G_2]$, the linear controller is represented by $K = [K_1\ K_2]$ where:

$$K(z) \sim \begin{cases} x_c(k+1) = A_c x_c(k) + B_c y_{lin}(k) + B_{cr} r(k) \\ u_{lin}(k) = C_c x_c(k) + D_c y_{lin}(k) + D_{cr} r(k) \end{cases} \tag{11}$$

$\Theta = [\theta_1\ \theta_2]$ is the AW controller becoming active only when saturation occurs. Given the difficulty in analyzing the stability and performance of this system we now adopt a framework first introduced in (Weston et al, 1998) for the problem at hand. This approach reduces to a linear time invariant Anti-Windup scheme that is optimized in terms of a transfer function: $M(z)$ shown in Figure 7 (b). It was shown in (Weston et al., 1998) that the performance degradation experienced by the system during saturation is directly related to the mapping T: $u_{lin} \rightarrow y_d$. Note that from Figure 7(b) $M - I$ is considered for stability of T and G_2M determines the systems recovery after saturation, where I is the identity matrix. This decoupled representation visibly shows how this mapping can be utilized as a performance measure for the AW controller. To quantify this we say that an AW controller is selected such that the L_2-gain, $||T||_{i,2}$, of the operator T:

$$\left\|T\right\|_{i,2} = \sup_{0 \neq u_{lin} \in L_2} \frac{\left\|y_d\right\|_2}{\left\|u_{lin}\right\|_2}$$

where the L_2 norm $||x||_2$ of a discrete signal $x(h)$, $(h = 0, 1, 2, 3, ...)$ is:

Figure 7. (a) A generic anti-windup scenario, (b) Weston Postlethwaite Anti-Windup conditioning technique

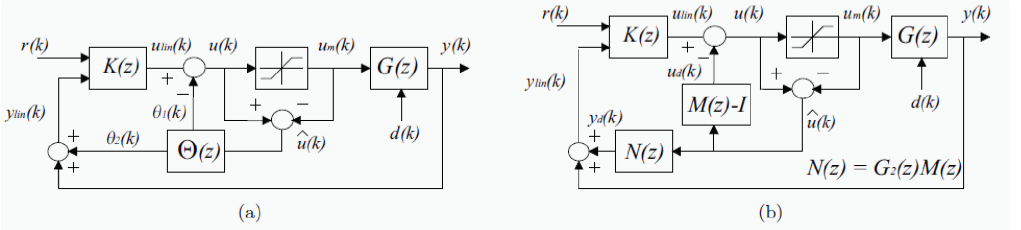

$$\|x\|_2 = \sqrt{\sum_{h=0}^{\infty} \|x(h)\|^2}$$

Static anti-windup synthesis: Static AW has an advantage in that it can be implemented at a much lower computational cost and adds no additional states to the closed loop system. Using the aforementioned conditioning technique via *M(z),* outlined in (Turner & Postlethwaite, 2004), Θ from Figure 7(a) is given by:

$$\begin{bmatrix} \theta_1 \\ \theta_2 \end{bmatrix} = \Theta\hat{u} = \begin{bmatrix} \theta_1 \\ \theta_2 \end{bmatrix} \hat{u}$$

u is derived from Figure 7(a) and Figure 7(b) respectively, as:

$$u = K_1 r + K_2 y - [(I - K_2 G_2)M - I\,]\,\hat{u}$$
$$u = K_1 r + K_2 y + (K_2 \Theta_2 - \Theta_1)\,\hat{u}$$

Thus *M(z)* can be written as:

$$M = (I - K_2 G_2)^{-1} (-K_2 \Theta_2 + \Theta_1 + I)$$

The goal of the static AW approach is therefore to ensure that extra modes do not appear in the system. Since this will inevitably be the case it must be ensured that minimal realizations of the controller and plant are used (Herrmann et al., 2007). A state space realization can be then formed:

$$\begin{bmatrix} M(z) - I \\ N(z) \end{bmatrix} \sim \begin{bmatrix} \dot{\bar{x}} \\ u_d \\ y_d \end{bmatrix} = \begin{bmatrix} \bar{A} & B_0 + \bar{B}\Theta \\ \bar{C}_1 & D_{01} + \bar{D}_1\Theta \\ \bar{C}_2 & D_{02} + \bar{D}_2\Theta \end{bmatrix} \begin{bmatrix} \bar{x} \\ \hat{u} \end{bmatrix} \tag{12}$$

where $\Theta = [\Theta'1_\Theta'2\,]'$ is a static matrix and *x, A, B_0, B, C_1, D_{01}, D_1, C_2,* D_{02} and D_2 are minimal realizations given in the Appendix. In a similar manner to (Herrmann et al., 2007), if there exist $Q > 0$, $U = diag(v_1, \cdots, v_c) > 0$ and *L* such that the following LMI is satisfied, then $||T||$ will be less than γ.

$$\begin{bmatrix} -Q & -Q\bar{C}_1' & Q\bar{A}' & 0 & -Q\bar{C}_2' \\ - & -X & UB_0 + L'\bar{B}' & I & UD'_{02} + L'\bar{D}_2' \\ - & - & -Q & 0 & 0 \\ - & - & - & -\gamma I & 0 \\ - & - & - & - & -\gamma I \end{bmatrix} < 0 \tag{13}$$

Where:

$$X = 2U + D_{01}U + \bar{D}'_1 L + UD'_{01} + L'\bar{D}'_1$$

and with $_{Q>0,\ U=diag(v1,\ldots vc)>0}$ $L \in \Re^{(c+n)\times n}$ (where c = n), the minimized L_2 gain $||T||_{i,2} < \gamma$ (where γ is the L_2 gain bound on *T*). The '-' entries in (13) are transpose conjugate of the corresponding entries to make the LMI symmetric. In this instance Θ is given by $\Theta = LQ^{-1}$ using which the controller in (12) can be synthesized. Ap-

plying this synthesis routine to our plant given by (5) and linear controller (9), the resultant controller is $\Theta = [-0.2049\ 0.6377]'$ obtained using the LMI toolbox in Matlab.

6. MODIFIED AWBT DESIGN

A. Motivation

To motivate the need for the proposed modification to the above AWBT technique, the reader is directed to Figure 6. As mentioned previously traditional AWBT schemes require that the feedback signal entering the "off-line" controller equals or is close in magnitude to the feedback signal entering the "on-line" controller. Clearly from Figure 6 this is not the case as $d_1(k) = d_2(k)$ due to differing propagation environments. As a result the AWBT controller in Figure 7(b) cannot guarantee the controller outputs for both the "off-line" and "on-line" controllers are equal in magnitude. The result can be an unwanted transient at switching due to the incompatible controller values, possibly causing vital health status information to be lost or a total breakdown in communication.

B. Proposed Solution

The following modification compensates for the inherent discrepancy in feedback RSSI signals between the "off-line" and the "on-line" controllers. Figure 8 illustrates the modification to the system. Consider the "off-line" controller base station 2, where an additional signal $y_{diff\,2}(k)$ is included in the feedback signal. This signal comprises of:

$$y_{diff\,2}(k) = -y_{online}(k)W(z) + y_{lin2}(k)W(z) \tag{14}$$

where $W(z)$ is a low pass filter removing the high frequency component present in each of the feedback RSSI signals. Note that $y_{online}(k)$ is determined by which base station is online. Therefore $y_{online}(k) = y_{lin1}$ given BS 1 is online. The signal driving the "off-line" controller then becomes:

$$y_{mod2}(k) = y_{lin2}(k) - y_{diff\,2}(k) = y_{lin2}(k) + y_{lin1}(k)W(z) - y_{lin2}(k)W(z)$$
$$y_{mod2}(k) = y_{lin1}(k)W(z) + y_{lin2}(k)(1 - W(z)) \tag{15}$$

which comprises of the "dc" or low frequency component of the "on-line" feedback signal or $y_{lin1}(k)W(z)$ and the high frequency component of the "off-line" control signal $y_{lin2}(k)(1-W(z))$. Each of these signals are incorporated in the design for different reasons. Firstly driving the "off-line controller" with the "dc" component of the "on-line" control signal will ensure both controller outputs will be approximately equal or $u_1(k) \approx u_2(k)$. Retaining the high frequency component of the "off-line" feedback signal enables the "off-line" controller with the ability to compensate for deep fades in its own feedback signal. Should power controller switching then occur a large transient is avoided as the feedback conditions are compatible.

Should base station 2 become "on-line" equation (15) becomes:

$$y_{mod2}(k) = y_{lin2}(k) - y_{diff\,2}(k) = y_{lin2}(k) + y_{lin2}(k)W(z) - y_{lin2}(k)W(z) = y_{lin2}(k) \tag{16}$$

hence the modification has no effect on the system and the AWBT scheme operates as normal. This approach in essence adds a filtered additional disturbance to the system which is intuitively appealing given a perturbation of the disturbance feedforward portion of the plant G_1 will have no bearing on stability (Turner et al., 2007). Taking into account the modification (11) can be rewritten as:

$$K(z) \sim \begin{cases} x_c(k+1) = \\ A_c x_c(k) + B_c y_{mod}(k) + B_{cr} r(k) \\ u_{lin}(k) = \\ C_c x_c(k) + D_c y_{mod}(k) + D_{cr} r(k) \end{cases} \tag{17}$$

Figure 8. The proposed modified WP-AW scheme, 2 Base Station Scenario

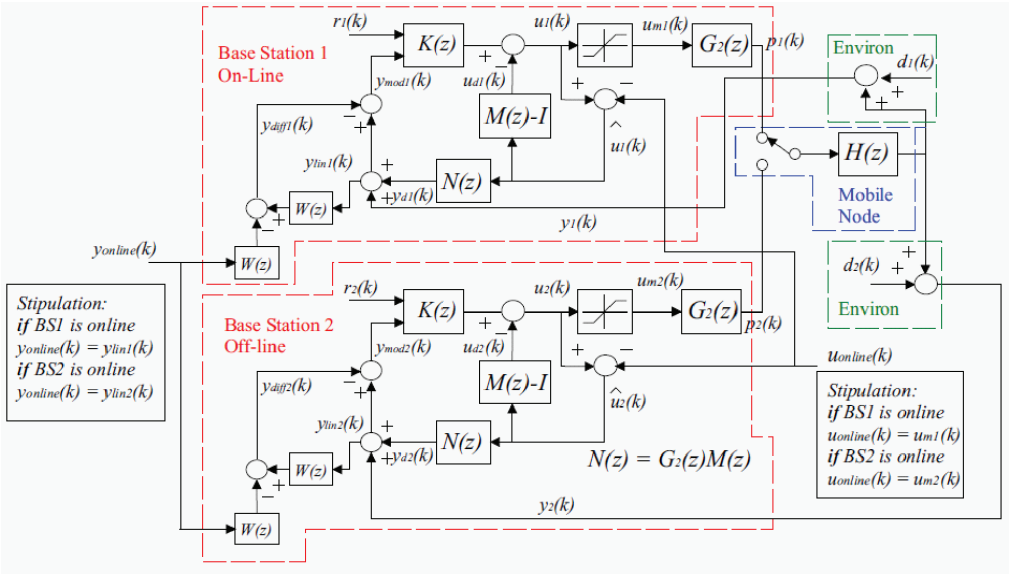

7. EXPERIMENTATION AND DISCUSSION

This section is organized as follows: Firstly a number of system parameters and performance criteria specific to this scenario are outlined. Some results are then presented to highlight the improvements afforded by the modified AWBT scheme ignoring the inherent saturation constraints. The fully scalable experimental testbed is then introduced. Finally a series of experiments are implemented on a fully compliant 802.15.4 wireless sensor testbed. In all cases the system response is analysed first without AWBT, then with the introduction of AWBT and finally with the modified AWBT design in place.

A. System Parameters and Performance Criteria

A sampling frequency of $T_s = 1(sec)$ is used throughout and a target RSSI value of −55dBm is selected for tracking, guaranteeing a PER of < 1%, verified using equations (3), (4) and (2).

The *standard deviation* of the RSSI tracking error is chosen as a performance criterion:

$$\sigma_e = \left\{ \frac{1}{S} \sum_{k=1}^{S} \left| r(k) - RSSI(k) \right|^2 \right\}^{\frac{1}{2}} \tag{18}$$

where S is the total number of samples and k is the index of these samples. *Outage probability* is defined as:

$$P_0(\%) = \frac{numberoftimesRSSI < RSSI_{th}}{thetota \ln umberofiterations} \times 100 \tag{19}$$

where $RSSI_{th}$ is selected to be −57dBm, a value below which performance is deemed unacceptable in terms of PER. This can be easily verified again using equations (2), (3) and (4). To fully access each paradigm, some measure of power efficiency is also useful and here we define average power consumption in milliwatts as:

$$P_{av} = 10^{\left[\left\{ \frac{1}{S} \sum_{k=1}^{S} p_{dBm}(k) \right\} / 10 \right]} (mW) \tag{20}$$

where $p_{dBm}(k)$ is the output transmission power in dBm, S is the total number of samples and k is the index of these samples.

B. Bumpless Transfer Performance

Due to the naturally occurring transceiver output power saturation nonlinearity in the system, which cannot be removed, it is difficult to ascertain the performance improvements afforded by the bumpless transfer as a standalone power controller switching scheme. Simulation can be a useful tool in this regard. Figure 9 illustrates some results were at time index 100 switchingoccurs between two base stations. In this instance there is a difference of 20 dBm in RSSI, between the signal received at the "online" base station and the RSSI signal observed at the "off-line" base station. As mentioned earlier this dissimilarity in observed RSSI is due to the propagation environment and is a realistic value based on experimental observations in an indoor environment. As a result of this feedback discrepancy the system without AWBT exhibits an extremely large transient response and indeed never achieves steady state prior to completion of the simulation. The system with AWBT in place shows improvement, however there is significant time spent below $RSSI_{th}$ and as a result outage probability is still at an unacceptable level. When the modified AWBT scheme is added the outage probability is dramatically reduced highlighting the improved performance afforded by the new scheme. The results in terms of the performance criteria are summarized in Table 2.

C. Experimental Testbed Description

To illustrate the use of the proposed algorithms in practice, a scaled experiment was formulated bridging the gap between simulation and implementation, an important step given the unpredictable nature of the wireless channel. The Tmote Sky mote sensor node is an

Figure 9. Modified AWBT performance ignoring saturation constraints and where power controller switching occurs at 100 (sec)

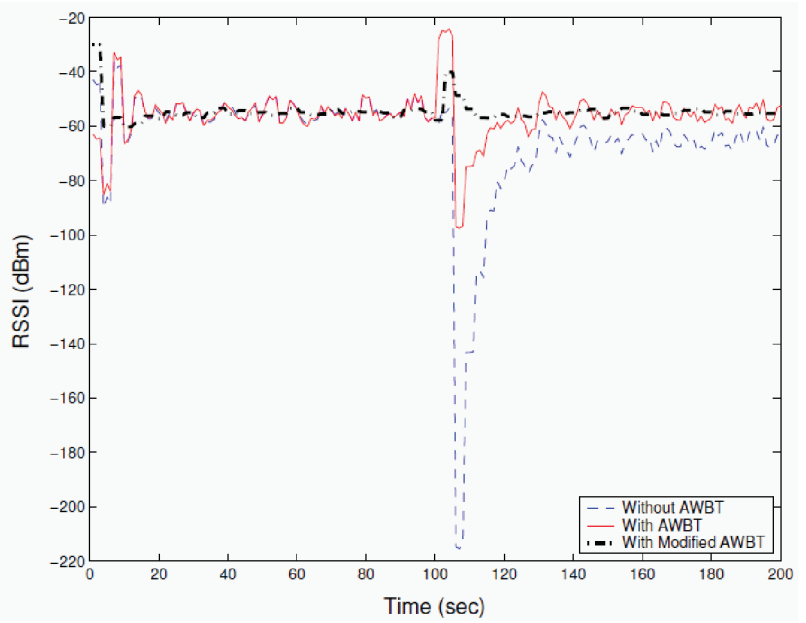

Table 2. Simulation results. Characteristics: σe - standard deviation (dbm), po - outage probability (%), pav - average power consumption (mw).

	Without AWBT	With AWBT	Modified AWBT
σe	30.59	4.445	1.603
Po	63.77	31.88	8.696
Pav	1	0.199	0.158

Figure 10. (a) Experimental Testbed Scenario, (b) Miabot pro with onboard Tmote Sky node

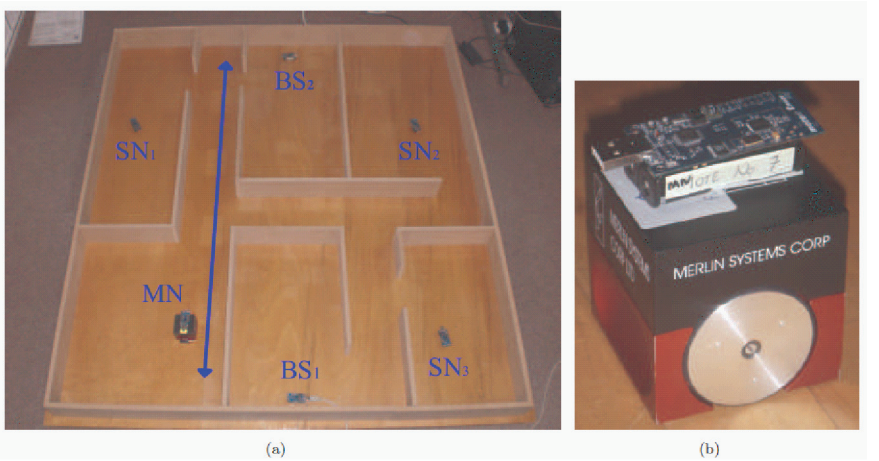

embedded platform using an 802.15.4 compliant transceiver and is selected as the primary embedded platform for this work. The Tmote platform employs the CC2420 transceiver using the Direct Sequence Spread Spectrum (DSSS) technique to code the biometric or accelerometer data. Carrier Sensing Multiple Access/Collision Avoidance (CSMA/CA) is then used to transmit the coded packets. The CC2420 transceiver on the Tmote platform provides a received signal strength indicator (RSSI) measurement in dBm by averaging the received signal power over 8 symbol periods or 128μs. Sensor data packets are framed in 802.15.4 format and transmitted using the TinyOS library function Oscope. The base station bridges packets over the USB/Serial connection to a personal computer where an interface between Matlab and TinyOS has been established using TinyOS Matlab tools written in Java.

The experimental setup shown in Figure 10(a), consists of a six Tmote nodes, two of which act as base stations or access points. A fully autonomous MIABOT Pro miniature mobile robot [23] is used to introduce mobility into the system, see Figure 10(b), to enable switching to occur. The first base station labeled BS_1 is connected to a PC and forwards all packets directly into the Matlab environment as discussed above. The second base station or BS_2 is a wireless device capable of gathering data from nodes within range and forwarding it in a multihop manner to BS_1 also known as the personal area network (PAN) coordinator. BS_2 is also capable of implementing power control for nodes located in lower tiers of the hierarchy as explained in the next section and

Figure 11. Experimental results where RSSI is the overall tracking signal, the dashed line is the saturated/actual controller output for base station 1 and the solid line is the saturated/actual controller output for base station 2. In this scenario, switching occurs at time $t \approx 60s$ and $t \approx 120s$. From above (a) System response without AWBT compensation, (b) System response with AWBT compensation, (c) System response with Modified AWBT compensation

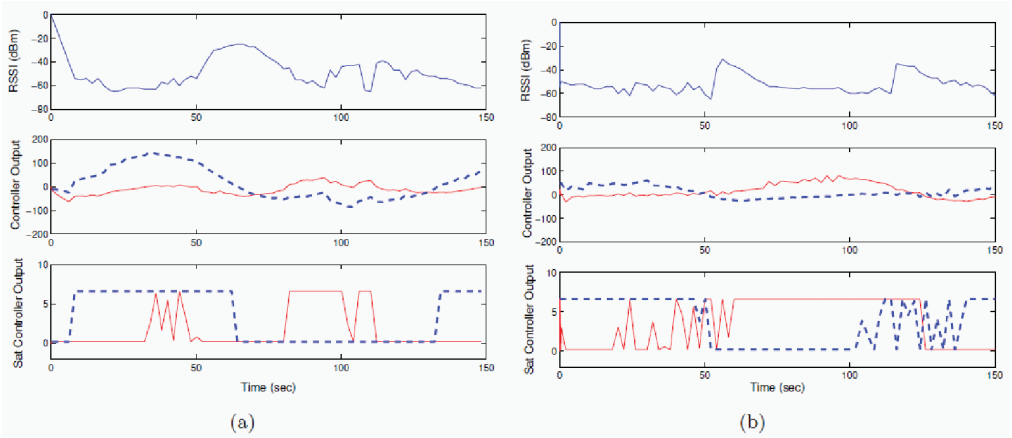

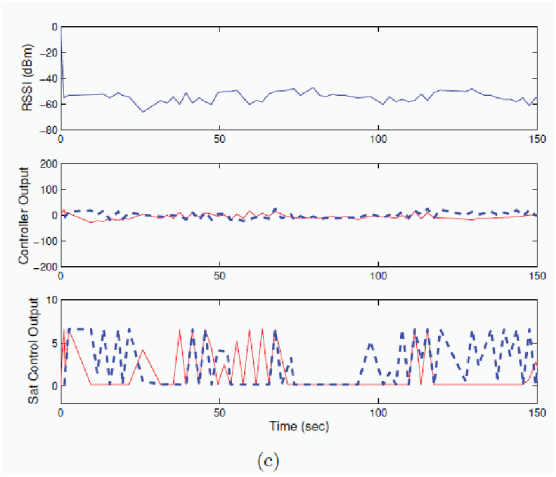

illustrated by Figure 2(a). The MIABOT robot has an additional Tmote, *MN*, onboard and follows a trajectory along which power controller switching occurs between BS_1 and BS_2. This is equivalent to a patient or elderly person in an ambulatory environment moving outside of the range of one access point and within range of another. Smooth switching between these two access points will ensure vital health status information is not lost. The additional stationary nodes SN_1, SN_2 and SN_3, introduce interference into the system providing for a more realistic scenario. For consistency the trajectory along which the mobile robot travels remains the same. For each experiment all relevant data both visual and numerical is recorded and stored for further analysis.

Figure 12. Results in terms of the performance criteria. Standard deviation has units dBm. Average power consumption is given in milliwatts

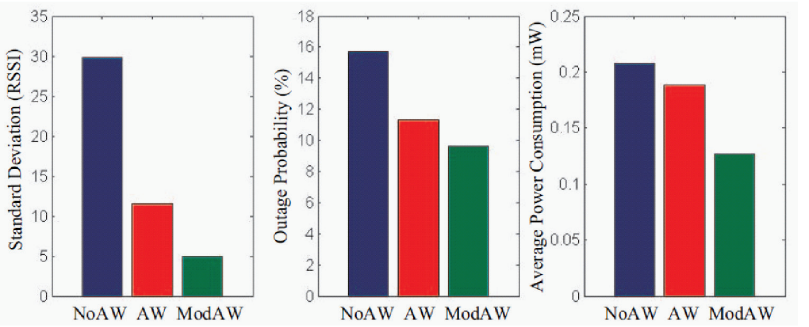

D. Experimental Results

Figure 11(a) illustrates the experimental system response without AWBT or with the control configuration shown in Figure 6. In this scenario, switching occurs at time $t \approx 60s$ and $t \approx 120s$. Clearly without AWBT there is significant integral windup in the system, keeping both the controller at BS_1 and at BS_2 saturated for the entire duration of the experiment and making it impossible for the system to track its reference RSSI accurately. In Figure 11(b) AWBT is added to the system and some improvement is observed in tracking performance, however upon closer inspection it is apparent when power controller switching occurs an undesirable transient is imposed on the system. The "off-line" controller output also exhibits an undesirable increase in magnitude, for instance the controller at BS_2 between 0 and 50 (sec). This is due to the discrepancy in the feedback signals or as $d_1(k) = d_2(k)$ (Figure 6) and results in excess power consumption in the network. The modified AWBT scheme almost eliminates this unwanted transient behaviour as shown in Figure 11(c) and this can be attributed to the modified compensators ability, when "off-line", to keep its control signal close in magnitude to the signal entering the plant despite the presence of ambiguity in the feedback signal. The results are summarized in Figure 12.

8. CONCLUSION

A novel Anti-Windup Bumpless Transfer (AWBT) scheme has been presented that enables smooth, power aware switching for networked wireless healthcare applications. The new technique facilitates the continual availability of biometric information in mesh networks that arise quite naturally in an ambulatory setting. Feedback discrepancies, hardware limitations and propagation phenomena that are posed by the use of commercially available wireless communication devices were addressed using new signal processing and robust anti-windup design tools. The approach was validated using a fully scalable 802.15.4 compliant wireless testbed. The new AWBT scheme exhibited significant performance improvements, particularly in terms of transient behaviour at power controller switching, when compared with analogous systems operating with simple dynamic control or when only Anti-Windup (AW) methods were applied in isolation. In future work the authors will apply the results presented here in a clinical study into fall detection and prevention for the elderly that will follow on from an EU Framework project in this application space.

9. ACKNOWLEDGMENT

The authors would like to acknowledge the support of Science Foundation Ireland under grant numbers 05/RFPCM/S0048 and 07/CE/I1147.

REFERENCES

Alavi, S. M. M., Walsh, M. J., & Hayes, M. J. (2009). Robust distributed active power control technique for IEEE 802.15.4 wireless sensor networks - a quantitative feedback theory approach. *Control Engineering Practice*, *17*(7), 805–814. doi:10.1016/j.conengprac.2009.02.001

Alavi, S. M. M., Walsh, M. J., & Hayes, M. J. (2010). Robust power control for IEEE 802.15.4 wireless sensor networks with round-trip time-delay uncertainty. *Wireless Communications and Mobile Computing*, *10*(6), 811–825.

Ares, B. Z., Fischione, C., Speranzon, A., & Johansson, K. H. (2007). On power control for wireless sensor networks: System model, middleware component and experimental evaluation. In *Proceedings of the* European Control Conference, Kos, Greece.

Bernstein, D. S., & Michel, A. N. (1995). A chronological bibliography on saturating actuators. *International Journal of Robust and Nonlinear Control*, *5*, 375–380. doi:10.1002/rnc.4590050502

Borghesani, C., Chait, Y., & Yaniv, O. (2003). *The QFT frequency domain control design toolbox for use with MATLAB*. Arlington Heights, IL: Terasoft.

Boulos, M. K., Rocha, A., Martins, A., Vicente, M. E., Bolz, A., & Feld, R. (2007). CAALYX: A new generation of location-based services in healthcare. *International Journal of Health Geographics*, *6*(1), 9. doi:10.1186/1476-072X-6-9

Chen, Y.-H., Lee, B.-K., & Chen, B.-S. (2006). Robust Hinf power control for CDMA cellular communication systems. *IEEE Transactions on Signal Processing*, *54*(10), 3947–3956. doi:10.1109/TSP.2006.880237

Gao, T., Pesto, C., Selavo, L., Chen, Y., Ko, J.-G., Lim, J.-H., et al. (2008). Wireless medical sensor networks in emergency response: Implementation and pilot results. In Proceedings of the IEEE International Conference on Technologies for Homeland Security, Waltham, MA (pp. 187-192).

Goldsmith, A. (2006). *Wireless communications*. Cambridge, UK: Cambridge University Press.

Hanus, R., Kinnaert, M., & Henrotte, J. (1987). Conditioning technique a general anti-windup and bumpless transfer method. *Automatica*, *23*, 729–739. doi:10.1016/0005-1098(87)90029-X

Herrmann, G., Turner, M., & Postlethwaite, I. (2006). Discrete-time and sampled-data anti-windup synthesis: stability and performance. *International Journal of Systems Science*, *37*(2), 91–114. doi:10.1080/00207720500444074

Herrmann, G., Turner, M., Postlethwaite, I., & Guo, G. (2004). Practical implementation of a novel anti-windup scheme in a HDD-dual-stage servo-system. *IEEE/ASME Transactions on Mechatronics*, *9*(3). doi:10.1109/TMECH.2004.835333

Horowitz, I. (2001). Survey of quantitative feedback theory (QFT). *International Journal of Robust Nonlinear Control*, *11*, 887–921. doi:10.1002/rnc.637

IEEE. Computer Society. (2006). *IEEE Std 802.15.4: Wireless lan medium access control (mac) and physical layer (phy) specifications for low-rate wireless personal area networks (lr-wpans)*. Washington, DC: IEEE Computer Society.

Srinivasan, K., & Levis, P. (2006). RSSI is under appreciated. In Proceedings of the Third Workshop on Embedded Networked Sensors EmNets.

Subramanian, A., & Sayed, A. H. (2005). Joint rate and power control algorithms for wireless networks. *IEEE Transactions on Signal Processing*, *53*(11), 4204–4214. doi:10.1109/TSP.2005.857044

Turner, M., Herrmann, G., & Postlethwaite, I. (2007). Incorporating robustness requirements into anti-windup design. *IEEE Transactions on Automatic Control*, *52*(10), 1842–1855. doi:10.1109/TAC.2007.906185

Turner, M., & Postlethwaite, I. (2004). A new perspective on static and low-order anti-windup synthesis. *International Journal of Control*, *77*, 27–44. doi:10.1080/00207170310001640116

Walsh, M. J., Alavi, S. M. M., & Hayes, M. J. (2008, December 9-11). On the effect of communication constraints on robust performance for a practical 802.15.4 wireless sensor network benchmark problem. In *Proceedings of the 47th IEEE Conference on Decision and Control*, Cancun, Mexico (pp. 447-452).

Walsh, M. J., Alavi, S. M. M., & Hayes, M. J. (2010). Practical assessment of hardware limitations on power aware wireless sensor networks- an anti-wind up approach. *International Journal of Robust and Nonlinear Control*, *20*(2), 194–208. doi:10.1002/rnc.1475

Walsh, M. J., Hayes, M. J., & Nelson, J. (2009). Robust performance for an energy sensitive wireless body area network - an anti-windup approach. *International Journal of Control*, *82*(1), 59–73. doi:10.1080/00207170801983109

Weston, P. F., & Postlewaite, I. (1998). Analysis and design of linear conditioning schemes for systems containing saturating actuators. In Proceedings of the IFAC Nonlinear Control System Design *Symposium*.

*Michael J. Walsh received a first class honors B.E. degree in Electronic Engineering from the University of Limerick in 2005. He subsequently applied for and was awarded a Ph.D. scholarship sponsored by the Embark Initiative's Postgraduate Research Scheme under the Irish Council for Science, Engineering and Technology (IRCSET). He completed his PhD, entitled "*An AntiWindup Approach to Reliable Communication and Resource Management in Wireless Sensor Networks*", as a member of the Wireless Access Research Centre in the Electronic and Computer Engineering Department at the University of Limerick in 2009. Following completion of his Ph.D., Michael joined the Tyndall National Institute in Cork, where he is currently a post-doctoral researcher funded by the Clarity Centre for Sensor Web Technologies. His research interests are presently centred on the development of wearable body area networks and more specifically the design and practical evaluation of new miniaturized heterogeneous wearable technologies. He is also concerned with protocol development for wireless body area networks, where his goal is to apply systems science and optimization techniques in the wireless ambient healthcare environment.*

John Barton received his M.S degree from University College Cork in 2006. He joined the Interconnection and Packaging Group of the National Microelectronics Research Centre (now Tyndall National Institute) as a research engineer in 1993. Currently in the Wireless Sensor Networks team where his recent research interests include ambient systems research, wearable computing and deployment of wireless sensor networks for personalized health applications. As PI on the Enterprise Ireland funded D-Systems project John has been the leader of the development of the Tyndall Wireless Sensor Mote platform. He has authored or co-authored over 90 peer reviewed papers.

Brendan O'Flynn received his B.E. degree from University College Cork in 1993, and his M.S. degree from University College Cork, National Microelectronics Research Centre in 1995. Brendan is a senior staff researcher at the Tyndall national Institute and is Research Activity Leader for the Wireless Sensor Network (WSN) Group. As such he has been responsible for directing the research activities of the group in a variety of industry funded, nationally funded and European projects. He has been involved in the development of the AES Intern Program, and conducting research into miniaturized wireless sensor systems as well as the supervision activities associated with postgraduate students PhD and Masters Level. His research interests include low power microelectronic design, RF system design system integration of miniaturized sensing systems and embedded system design on resource constrained platforms. Brendan was one of the founders of Inpact Microelectronics Ireland Ltd. and has significant expertise in the commercialization of technology. Inpact (a spin off from the National Microelectronics Research Centre (NMRC)) miniaturized in the development of system in a package (SiP) solutions for customers. Inpact offered a complete solution to customers enabling the development of a product concept through to volume product supply; miniaturizing in radio frequency (RF) system development and product miniaturization.

Martin J. Hayes has lectured at the University of Limerick since 1997, is currently course leader for the B.S. in Electronics programme, and is a researcher in the Wireless Access Research Centre. He teaches undergraduate and postgraduate courses in electrical science, automatic control, computer controlled systems and the control of nonlinear systems. His research interests lie in the area of systems theory in general and in particular on the intelligent use of system resources within biomedical or safety critical wireless systems that are subjected to channel and/or performance uncertainties. He is also interested in how the dynamic delivery of information to handheld devices at tourist attractions can add value to the visitor experience.

Cian O'Mathuna is head of Tyndall National Institutes Microsystems Centre. His research interests include microelectronics integration for ambient electronic systems, biomedical microsystems, and energy processing for information and communications technologies. He received his PhD in Microelectronics from University College Cork. He is a member of the IEEE.

Seyed Mohammad Mahdi Alavi received his Bachelor and Master degrees in Control Engineering from K.N. Toosi University of Technology in 2001 and 2003, respectively and Ph.D. from University of Limerick, Ireland in 2009. He is currently a post doctorate researcher at Simon Fraser University, BC, Canada. His research interests include robust control theory (in particular Quantitative Feedback Theory) and fault detection and isolation technique with applications to wired/wireless networks as well as power systems. He received the best student award from K.N. Toosi University of Technology (2001); PhD scholarship from Science Foundation Ireland (May 2006–October 2008). He has held visiting positions at Centre for Embedded Software System, Aalborg University, Denmark (February–April 2007), and at Automatic Control Laboratory, EPFL, Switzerland (May–October 2007).

APPENDIX

Static Minimal Realizations

Given the state space realization of the plant:

$$\left[G_1 G_2\right] \sim \begin{bmatrix} A_p & B_{pd} B_p \\ C_p & D_{pd} D_p \end{bmatrix}$$

then the minimal realization is given by:

$$\bar{x} = \begin{bmatrix} x_p \\ x_c \end{bmatrix}, \bar{A} \sim \begin{bmatrix} A_p + B_p \tilde{\Delta} D_c C_p & B_p \tilde{\Delta} C_c \\ B_c \Delta C_p & Ac + B_c \Delta D_p C_c \end{bmatrix}$$

$$B_0 = \begin{bmatrix} B_p \tilde{\Delta} \\ B_c \Delta D_p \end{bmatrix}, \bar{B} \sim \begin{bmatrix} B_p \tilde{\Delta} & -B_p \tilde{\Delta} D_c \\ B_c \Delta D_p & -B_c \Delta \end{bmatrix}$$

$$\bar{C}_1 = \left[\tilde{\Delta} D_c C_p \quad \tilde{\Delta} C_c\right], D_{01} = \tilde{\Delta} D_c D_p, \bar{D}_1 = \left[I + \tilde{\Delta} D_c D_p \quad -\tilde{\Delta} D_c\right]$$

$$\bar{C}_2 = \left[\Delta C_p \quad \Delta D_p C_c\right], D_{02} = \Delta D_p, \bar{D}_2 = \left[\Delta D_p \quad -\tilde{\Delta} D_p D_c\right]$$